Pressure-induced electron transfer in ferrimagnetic Prussian blue analogs

Vadim Ksenofontov,* Georgiy Levchenko, Sergey Reiman, and Philipp Gütlich
Institut für Anorganische Chemie und Analytische Chemie, Johannes Gutenberg-Universität, Staudinger Weg 9, D-55099 Mainz, Germany

Anne Bleuzen, Virginie Escax, and Michel Verdaguer
Laboratoire de Chimie Inorganique et Matériaux moléculaires, Unité CNRS 7071, Université Pierre et Marie Curie, Bât F 74, 4 place Jussieu, 75252 Paris Cedex 05, France

(Received 27 May 2002; revised manuscript received 11 February 2003; published 28 July 2003)

Mössbauer and magnetic susceptibility measurements were performed under pressure on three Prussian blue analogs, $K_{0.1}Co_4[Fe(CN)_6]_{2.7}\cdot 18H_2O$, $K_{0.28}Co_4[Fe(CN)_6]_{2.76}\cdot 18H_2O$, and $Cs_{0.7}Co_4[Fe(CN)_6]_{2.9}\cdot 16H_2O$. A pressure-induced electron transfer $Co^{2+}(S=\frac{3}{2})$-$Fe^{3+}(S=\frac{1}{2})\rightarrow Co^{3+}(S=0)$-$Fe^{2+}(S=0)$ was found. The ''scanning'' of the ligand field strength by applying an external hydrostatic pressure allows the exploration of the distribution of CoN_nO_{6-n} $(0\leqslant n\leqslant 6)$ configurations. It reveals a narrow distribution of configurations centered around the most probable CoN_4O_2 configuration in $K_{0.1}Co_4[Fe(CN)_6]_{2.7}\cdot 18H_2O$ and a broad CoN_nO_{6-n} distribution in $K_{0.28}Co_4[Fe(CN)_6]_{2.76}\cdot 18H_2O$ and $Cs_{0.7}Co_4[Fe(CN)_6]_{2.9}\cdot 16H_2O$. This evolution of site distribution caused by alkali doping, explored here for the first time, to our knowledge is shown to play an important role in the photoinduced magnetization process.

DOI: 10.1103/PhysRevB.68.024415 PACS number(s): 75.50.Gg, 75.30.Kz, 74.62.Dh, 74.62.Fj

I. INTRODUCTION

In 1996, Hashimoto and co-workers found a photoinduced magnetization (PIM) effect in a cobalt-iron Prussian blue analog.[1] They explained the phenomenon by the presence of diamagnetic low spin Co^{3+}-Fe^{2+} pairs and a photoinduced electron transfer from Fe^{2+} to Co^{3+} through the cyanide bridge to produce high spin Co^{2+}–low spin Fe^{3+} magnetic pairs.[2] This hypothesis was fully confirmed experimentally later on.[3–6]

The synthesis of the powdered samples can be described as substitution reactions of the water molecules of the hexaaqua complex $[Co^{2+}(H_2O)_6]^{2+}$ by $[Fe^{3+}(CN)_6]^{3-}$. In the face-centered cubic (*fcc*) structure of a Prussian blue analog such as $Co_4[Fe(CN)_6]_{8/3}\square_{4/3}\cdot xH_2O$, the stoichiometry implies that 33% of the $[Fe(CN)_6]$ sites are replaced by vacancies ($\square$) where the water molecules coordinated to the cobalt ions [Figs. 1(a) and 1(b)] give rise to an average CoN_4O_2 surrounding of the metal with four nitrogen (from cyanide) and two oxygen atoms (from water). By introducing various quantities of alkali metal cations M^+ in the tetrahedral sites of the *fcc* structure, the average environment of the cobalt ions changes up to $Co(NC)_6$ (six nitrogen atoms from the cyanide) in the compact structure $M_4Co_4[Fe(CN)_6]_4$ [Fig. 1(c)].[1,7,8]

Since the discovery of PIM, much effort has been devoted to the explanation of the appearance of diamagnetic pairs and the role of the vacancies in the PIM process.[3–6,9–12] A clear conclusion is that the progressive replacement of oxygen atoms from water by nitrogen atoms from cyanides increases the ligand field strength experienced by the cobalt ions, thereby destabilizing the two antibonding e_g^* electrons and the high spin state and strongly enhancing the cobalt reducing power. The consequence is a ''chemically'' (or ''structurally'') induced electron transfer from cobalt(II) to iron(III), leading to the more stable diamagnetic Co^{3+}-Fe^{2+} pair. The process may be represented as $Co^{2+}(S=\frac{3}{2})$-$Fe^{3+}(S=\frac{1}{2})\rightarrow[Co^{2+}(S=\frac{1}{2})$-$Fe^{3+}(S=\frac{1}{2})]\rightarrow Co^{3+}(S=0)$-$Fe^{2+}$ $(S=0)$.

A study of the charge transfer was undertaken in systems in which the amount and nature of the alkali cation were varied.[3] It was shown that the presence of diamagnetic pairs is necessary to observe a photo-induced magnetization. X-ray absorption spectroscopy measurements at the Co and Fe $L_{2,3}$ edges, XANES and EXAFS studies of cobalt *K*-edge indicate the local electronic transfer and the spin change of the cobalt ions induced by irradiation in $Rb_{1.8}Co_4[Fe(CN)_6]_{3.30}\cdot 13H_2O$.[4] A 0.19-Å mean increase of the Co-N(O) bond length is associated with the transformation of $Co^{3+}(S=0)$ to $Co^{2+}(S=\frac{3}{2})$.[4] In all instances, only the transformation $Co^{2+}(S=\frac{3}{2})$-$Fe^{3+}(S=\frac{1}{2})\rightarrow Co^{3+}(S=0)$-$Fe^{2+}(S=0)$ was revealed in these experiments and the

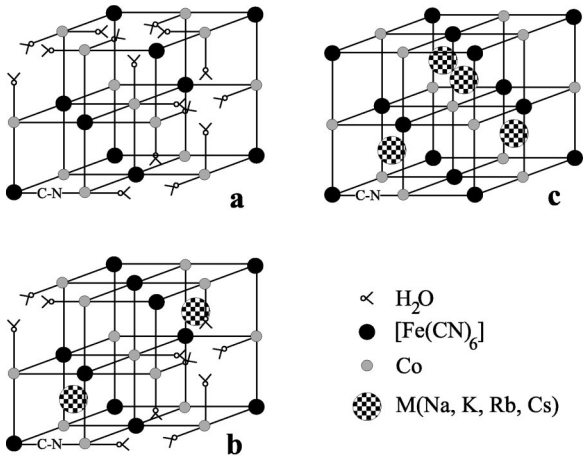

FIG. 1. Structure of Prussian blue analog $M_xCo_4[Fe(CN)_6]_{(8+x)/3}\cdot nH_2O$ (M is an alkali cation): (a) with $x=0$ and 33% of stoichiometrical vacancies filled with water molecules; (b) with $x=2$; (c) $x=4$, compact structure $M_4Co_4[Fe(CN)_6]_4$.

appearance of the possible $Co^{2+}(S=\frac{1}{2})$-$Fe^{3+}(S=\frac{1}{2})$ intermediate state, with a low spin cobalt(II), was never observed and its involvement remains an open question.

Another unanswered question associated with the photomagnetic properties in Co-Fe Prussian blue analog concerns of the distribution of the first coordination sphere of cobalt atoms. If one assumes a random distribution of $CoN_nO_{6-n}(0\leqslant n\leqslant 6)$ configurations in the two compounds $Cs_{0.7}Co_4[Fe(CN)_6]_{2.9}\cdot 6H_2O$ (hereafter abbreviated as $Cs_{0.7}Co_4Fe_{2.9}$) showing PIM and $K_{0.1}Co_4[Fe(CN)_6]_{2.7}\cdot 18H_2O$ (hereafter $K_{0.1}Co_4Fe_{2.7}$) showing no detectable PIM,[3,5,13] one cannot find any significant difference between them. Both compounds with 27.5%, and 32.5% vacancies, respectively, should have similar concentrations of ''strong-field'' configurations CoN_6 (and ''intermediate-field'' configuration CoN_5O), providing for the existence of the diamagnetic pairs $Co^{3+}(S=0)$-$Fe^{2+}(S=0)$, that is a necessary condition for PIM. With a binomial distribution, 9.5% CoN_6 and 27.3% CoN_5O configurations for $K_{0.1}Co_4Fe_{2.7}$, and 14.5% CoN_6 and 33.0% CoN_5O configurations for $Cs_{0.7}Co_4Fe_{2.9}$ are expected. On the basis of this model, the absence of the PIM effect in $K_{0.1}Co_4[Fe(CN)_6]_{2.7}\cdot 18H_2O$ cannot be understood. To clarify the role of alkali metal ion doping in the appearance of diamagnetic pairs and to provide a deeper understanding of the charge transfer process in Co-Fe Prussian blue analogs, we have studied the magnetic properties of $K_{0.1}Co_4Fe_{2.7}$, $K_{0.28}Co_4[Fe(CN)_6]_{2.76}\cdot 18H_2O$ (hereafter $K_{0.28}Co_4Fe_{2.76}$) and $Cs_{0.7}Co_4Fe_{2.9}$ under hydrostatic pressure, which provides a direct means of altering the ligand field strength without changing the chemical composition. In the three compounds under study the Co/Fe ratios are 1.48, 1.45, and 1.38, whereas the PIM effect in *K*-doped compounds is observed for Co/Fe ratios in the range 1.4–1.2.[14] ^{57}Fe Mössbauer spectroscopy under hydrostatic pressure was used as the probe of the electronic state of the iron sites.

II. EXPERIMENT

Sample preparation and characterization

The compounds $K_{0.1}Co_4Fe_{2.7}$, $K_{0.28}Co_4Fe_{2.76}$, and $Cs_{0.7}Co_4Fe_{2.9}$ were synthesized and characterized by elemental analysis, infra-red spectroscopy, X-ray absorption spectroscopy, and powder X-ray diffraction, as described in Refs. 3 and 5.

Mössbauer and magnetic susceptibility measurements under hydrostatic pressure

The variable-temperature magnetic susceptibility measurements of $K_{0.1}Co_4Fe_{2.7}$ and $Cs_{0.7}Co_4Fe_{2.9}$ were performed using the PAR 151 Foner-type magnetometer, equipped with a cryostat operating in the temperature range 2–300 K. The measurements of $K_{0.28}Co_4Fe_{2.76}$ were performed with a Quantum Design MPMS-XL superconducting quantum interference device magnetometer. The hydrostatic pressure cell made of hardened beryllium bronze with silicon oil as the pressure transmitting medium operates in the pressure range $1\ \text{bar}<P<13$ kbar, and its construction and application has been described elsewhere.[15] The dimensions of the cylindrically shaped powder sample holder dimensions are 1 mm in diameter and 5–7 mm in length. The pressure was measured using the pressure dependence of the superconducting transition temperature of a built-in pressure sensor made of high purity tin. Experimental data were corrected for diamagnetism using Pascal's constants.

^{57}Fe Mössbauer spectra were recorded using a conventional constant-acceleration spectrometer and a helium bath cryostat. Powder samples were measured in a Mössbauer pressure cell made of hardened beryllium bronze equipped with windows made of B_4C and with silicon oil as the pressure transmitting medium. The construction enables hydrostatic pressure measurements to be carried out up to 15 kbar in the temperature range 2–350 K. The Mössbauer pressure cell was calibrated using FeF_3 in accordance with published results.[16] The Recoil 1.02 Mössbauer Analysis Software was used to fit the experimental spectra.[17] Isomer shift values are quoted relative α-Fe at 293 K.

Experimental results

The $\chi_m T$ versus T plots of the three samples measured at ambient and under applied hydrostatic pressure are displayed in Fig. 2. The compound $K_{0.1}Co_4Fe_{2.7}$ shows at ambient pressure an antiferromagnetic interaction and a ferrimagnetic ordering below $T_C\cong 16$ K in accordance with published data.[18] This magnetic behavior remains unaltered as pressure is increased up to 3.0 kbar [Fig. 2(a)]. Drastic changes are observed as the pressure reaches 4.0 kbar. At this pressure in the temperature range $200\ \text{K}<T<300$ K a strong decrease of the $\chi_M T$ product is observed and at low temperature the long range magnetic ordering disappears. When the pressure is increased, the pressure-induced feature in the magnetic behavior above 200 K shifts to higher temperatures with a rate $\cong 17$ K/kbar. An important feature is that above the ''switching'' pressure of 4.0 kbar all magnetic curves in the low-temperature region almost coincide and are no longer influenced by further increase of pressure. At 10.2 kbar, in the temperature range 4.2–300 K, the $\chi_m T$ value varies from 3 to 5 $\text{cm}^3\,\text{mol}^{-1}\,\text{K}$.

The $\chi_m T$ vs T curve of $Cs_{0.7}Co_4Fe_{2.9}$ reveals at ambient pressure the coexistence of ferrimagnetic ordering and a feature similar to that described above for $K_{0.1}Co_4Fe_{2.7}$ at $P>4.0$ kbar [Fig. 2(b)]. Furthermore, in contrast to $K_{0.1}Co_4Fe_{2.7}$, the application of even the small pressure of 0.7 kbar causes a significant shift of the feature in the magnetic behavior above 200 K upwards and a decrease of the residual low-temperature value of $\chi_M T$; simultaneously, the intensity of the cusp-shape peak associated with magnetic ordering decreases. Further increase of pressure not only shifts the feature in the $\chi_m T$ vs T curve to higher temperatures, but monotonically decreases the residual low-temperature baseline, contrary to what happens in $K_{0.1}Co_4Fe_{2.7}$. The $\chi_m T$ vs T curve at pressure 8.1 kbar shows no sign of magnetic ordering at low temperature and is similar to the curve for $K_{0.1}Co_4Fe_{2.7}$ at $P=10.2$ kbar. A release of pressure reveals no irreversible change in both samples.

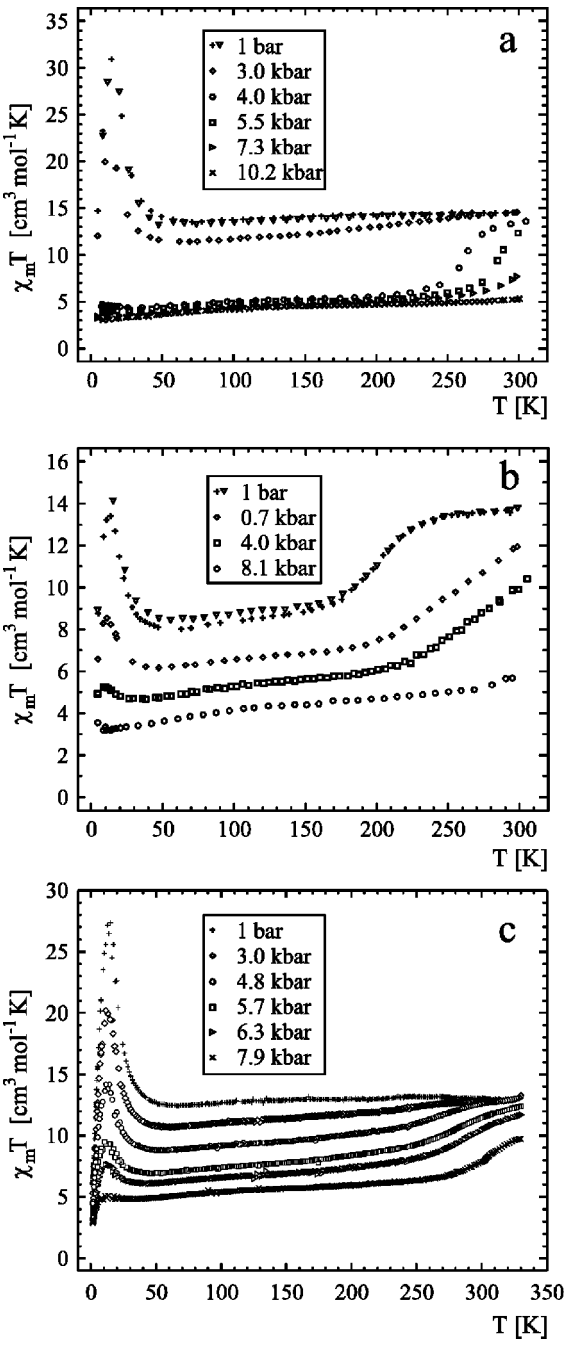

FIG. 2. Temperature dependence of $\chi_m T$ for $K_{0.1}Co_4Fe_{2.7}$ (a), $Cs_{0.7}Co_4Fe_{2.9}$ (b), and $K_{0.28}Co_4Fe_{2.76}$ (c) at different pressures. Measurements at 1 bar after release of pressure reveal a reversible behavior in the samples.

The behavior of the compound $K_{0.28}Co_4Fe_{2.76}$ at ambient pressure is similar to that of $K_{0.1}Co_4Fe_{2.7}$ [Fig. 2(c)]. However, the pressure-induced feature in the $\chi_m T$ vs T curve above 200 K appears to be gradual. Moreover, the residual baseline of the magnetic curve decreases monotonically with increase of pressure, similar to that for $Cs_{0.7}Co_4Fe_{2.9}$. At pressure 7.9 kbar low-temperature magnetic ordering disappears.

The magnetic susceptibility data refer to all atoms in the bulk sample and thus unequivocal interpretation of them in terms of the properties of the individual metal atoms is not feasible. On the other hand, the ^{57}Fe Mössbauer spectroscopic data are of microscopic nature and refer to iron sites only. At ambient pressure and 4.2 K the magnetically split Mössbauer spectrum confirms the magnetic ordering in $K_{0.1}Co_4Fe_{2.7}$ below 16 K, which was already established by magnetic susceptibility measurements [Fig. 3(a)].[18] The spectrum with an average hyperfine field $\langle H\rangle = 164(2)$ kOe and isomer shift $\delta = -0.07(2)$ mm/s corresponds to 100% of Fe^{3+} in the $S=\frac{1}{2}$ spin state. At a pressure of 3.0 kbar, in addition to the magnetically split spectrum, characteristic for $K_{0.1}Co_4Fe_{2.7}$ at ambient pressure, a contribution due to the diamagnetic $Fe^{2+}(S=0)$ component appears. This is the only iron species present at pressures exceeding 4.0 kbar (Fig. 4). A pressure-induced internal redox process $Fe^{3+}(S=\frac{1}{2}) \rightarrow Fe^{2+}(S=0)$ is clearly seen in the Mössbauer spectra at room temperature (Fig. 5). The appearance of Fe^{2+} leads to the asymmetry of the Mössbauer spectra of $K_{0.1}Co_4Fe_{2.7}$. At a pressure of 6.0 kbar there is 30(2)% of Fe^{2+}[$\delta = -0.15(1)$ mm/s quadrupole splitting $\Delta E_Q = 0.15(2)$ mm/s] present in addition to Fe^{3+} [$\delta = -0.22(2)$ mm/s, $\Delta E_Q = 0.51(5)$ mm/s].

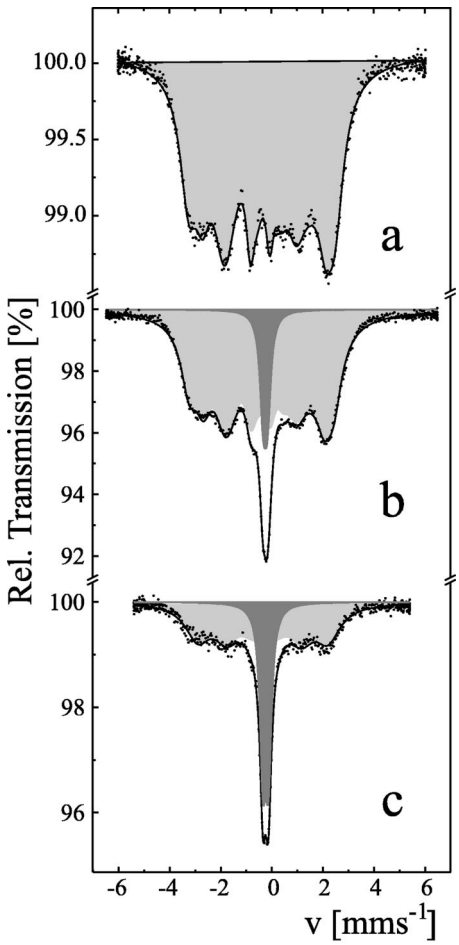

FIG. 3. Mössbauer spectra of $K_{0.1}Co_4Fe_{2.7}$ (a), $K_{0.28}Co_4Fe_{2.76}$ (b), and $Cs_{0.7}Co_4Fe_{2.9}$ (c) recorded at 4.2 K and ambient pressure. Shaded subspectra correspond to: $Fe^{2+}(S=0)$ (dark gray), and $Fe^{3+}(S=\frac{1}{2})$ (light gray).

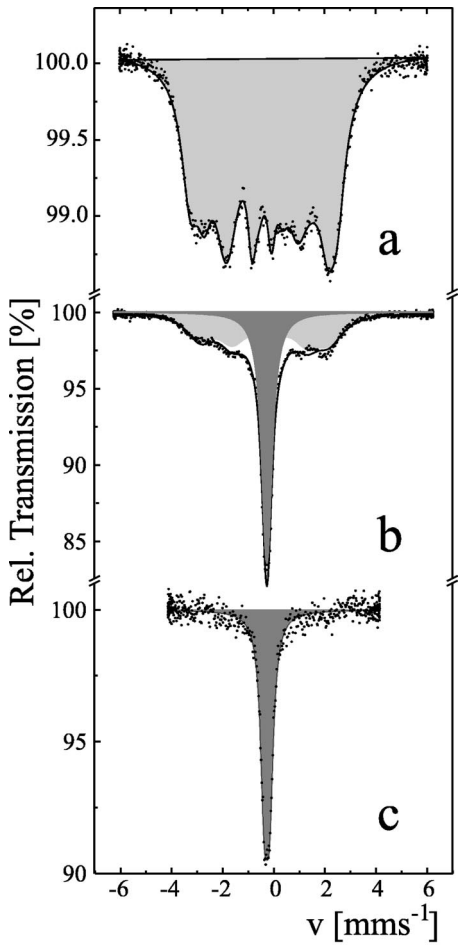

FIG. 4. Mössbauer spectra of $K_{0.1}Co_4Fe_{2.7}$ recorded at 4.2 K and different pressures: (a) 1 bar, (b) 3.0 kbar, and (c) 4.0 kbar. Shaded subspectra correspond to $Fe^{2+}(S=0)$ (dark gray), $Fe^{3+}(S=\frac{1}{2})$ (light gray).

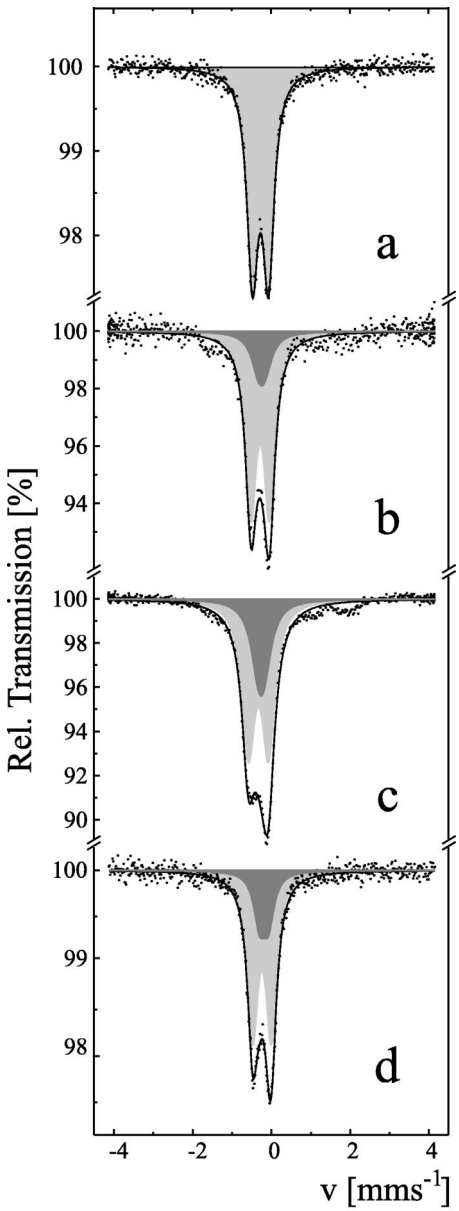

FIG. 5. Mössbauer spectra of $K_{0.1}Co_4Fe_{2.7}$ recorded at 293 K and different pressures: (a) 1 bar; (b) 4.0 kbar; (c) 6.0 kbar; (d) Mössbauer spectrum of $Cs_{0.7}Co_4Fe_{2.9}$ at ambient pressure and $T=293$ K. Shaded subspectra correspond to $Fe^{2+}(S=0)$ (dark gray) and $Fe^{3+}(S=\frac{1}{2})$ (light gray).

The Mössbauer spectrum of $K_{0.28}Co_4Fe_{2.76}$ at 4.2 K [Fig. 3(b)] consists of the magnetic component and a slightly broadened single line with relative intensity of 10(1)%. The magnetic subspectrum with $\langle H\rangle=161(1)$ kOe and $\delta=-0.06(1)$ mm/s originates from Fe^{3+}, whereas the single line with $\delta=-0.015(1)$ mm/s is attributed to low-spin Fe^{2+} to the extent of 10(1)%. It should be noted, that the fraction of diamagnetic Fe^{2+} in $K_{0.28}Co_4Fe_{2.76}$ is temperature independent. In Mössbauer experiments combined with light irradiation similar to those described in Refs. 11 and 19, we found no noticeable light-induced changes of the Fe^{3+}/Fe^{2+} ratio, which indicates the absence of PIM.

The low-temperature spectrum of $Cs_{0.7}Co_4Fe_{2.9}$ [Fig. 3(c)] similar to that of $K_{0.28}Co_4Fe_{2.76}$ consists of two components. The magnetically split subspectrum with $\langle H\rangle=158(1)$ kOe corresponds to low-spin Fe^{3+}. The amount of low-spin Fe^{2+} derived from the corresponding subspectrum area is 32(1)% of the total iron. It is important to notice that both Fe^{3+} and Fe^{2+} components coexist at room temperature in the spectrum of $Cs_{0.7}Co_4Fe_{2.9}$ at ambient pressure [Fig. 5(d)], the concentration of Fe^{2+} ions being 25(7)%, in fair agreement with previous evaluations.[4] Mössbauer pressure studies of $Cs_{0.7}Co_4Fe_{2.9}$ were done at 4.2 K. We found that a pressure of 1.5 kbar transforms $Fe^{3+}(S=\frac{1}{2})$ almost completely into $Fe^{2+}(S=0)$. The temperature dependence of the Fe^{3+} fraction in $K_{0.1}Co_4Fe_{2.9}$ at different pressures and in $Cs_{0.7}Co_4Fe_{2.9}$ at ambient pressure is shown in Fig. 6. The clear correlation of this quantity with the behavior of the magnetic susceptibility (Fig. 2) under pressure indicates, that the feature in the magnetic behavior observable above 200 K is caused by a pressure-induced charge transfer. This fact provides a basis for the interpretation of the pressure-induced processes in all three compounds under study.

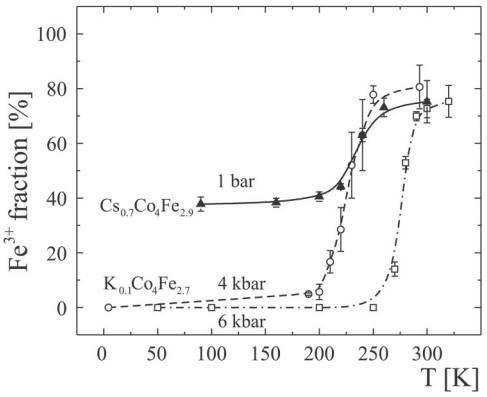

FIG. 6. Temperature dependence of the Fe^{3+} fraction in $K_{0.1}Co_4Fe_{2.7}$ at different pressures and in $Cs_{0.7}Co_4Fe_{2.9}$ at ambient pressure obtained from Mössbauer data.

III. DISCUSSION

The joint study of the magnetic properties and hyperfine interactions by Mössbauer spectroscopy under pressure in $K_{0.1}Co_4Fe_{2.7}$ provides clear evidence of pressure-induced electron transfer $Co^{2+}(S=\frac{3}{2})$-NC-$Fe^{3+}(S=\frac{1}{2})\rightarrow Co^{3+}(S=0)$-NC-$Fe^{2+}(S=0)$. Important features of the process are the narrow ($\leqslant$ 1 kbar) pressure interval necessary for complete transition and the existence of a threshold pressure (ca. 3 kbar). A pressure of more than 4.0 kbar transforms 100% of iron Fe^{3+} ions into Fe^{2+} and consequently an equal amount of cobalt Co^{2+} into Co^{3+} ions. From this observation and from the residual value of $\chi_M T$ after electron transfer (Fig. 2), it can be deduced that the spin state of the remaining 32.5% of Co^{2+} atoms, not involved in the electron transfer, is $S=\frac{3}{2}$ rather than the hypothetical intermediate low spin state $S=\frac{1}{2}$.[20] This means that an increase in the ligand field strength is a necessary, but not a sufficient condition to change the spin state of these cobalt centers. If one assumes a random distribution of configurations, the remaining Co^{2+} atoms may belong to the configurations CoN_nO_{6-n} on the ''weak ligand field'' side ($n\leqslant 3$) of the binomial distribution shown in Fig. 7. However, the result of ''scanning'' the ligand field strength by varying the external pressure indicates a narrower distribution of ligand field strengths (i.e., CoN_nO_{6-n} configurations), than that deduced from statistical considerations. Thus the CoN_4O_2 configuration predominates in $K_{0.1}Co_4Fe_{2.7}$ and is distributed in its crystal lattice in a quite regular way, i.e., the $K_{0.1}Co_4Fe_{2.7}$ has an essentially ordered structure. The proposed distribution of local configurations centered around CoN_4O_2 is presented in Fig. 7. The presence of residual $Co^{2+}(S=\frac{3}{2})$ ions at pressures greater than 4.0 kbar proves that the change in ligand field strength felt by the cobalt atoms does not occur if it is not accompanied by the charge transfer Co^{2+}-$Fe^{3+}\rightarrow Co^{3+}$-$Fe^{2+}$.

The amount of 25(7)% of Fe^{2+} found from the Mössbauer measurements of $Cs_{0.7}Co_4Fe_{2.9}$ at ambient pressure and room temperature is larger than the amount of CoN_6 (14.5%), but smaller than the total amount of CoN_6 and CoN_5O (47.5%) configurations, estimated from the model of a binomial distribution. However, the result of pressure ''scanning'' of ligand field strength in $Cs_{0.7}Co_4Fe_{2.9}$ reveals a broad distribution of configurations. The hypothetical binomial distribution of CoN_nO_{6-n} configurations taking into account the amount of low-spin Fe^{2+} species found at ambient pressure and room temperature is shown in Fig. 7. The presence of strong-field CoN_6 configurations at ambient pressure provides the same amount of diamagnetic pairs $Co^{3+}(S=0)Fe^{2+}(S=0)$, which are required for the PIM phenomenon. Mössbauer pressure studies of $Cs_{0.7}Co_4Fe_{2.9}$ confirmed the high sensitivity of the Fe^{3+}/Fe^{2+} ratio to the pressure in agreement with magnetic susceptibility measurements.

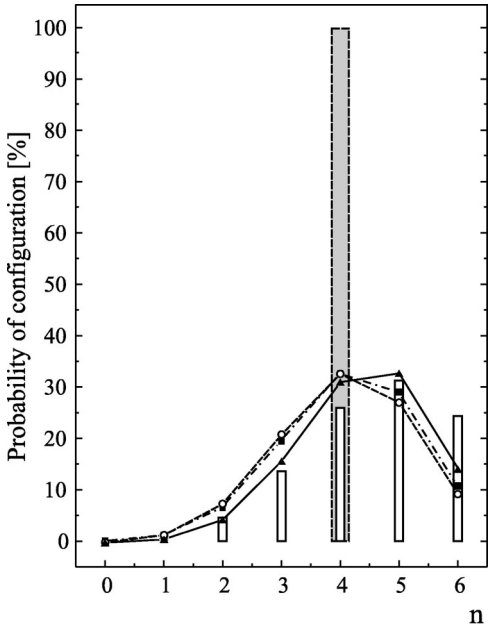

FIG. 7. Probability of CoN_nO_{6-n} ($0\leqslant n\leqslant 6$) configurations in $Cs_{0.7}Co_4Fe_{2.9}$ (closed triangles), $K_{0.28}Co_4Fe_{2.76}$ (closed squares), and $K_{0.1}Co_4Fe_{2.7}$ (opened circles) assuming a binomial distribution. The proposed distribution of configurations for $K_{0.1}Co_4Fe_{2.7}$ shown as shaded bulk is much more narrow than follows from the statistical model, whereas the proposed distribution of CoN_nO_{6-n} configurations in $Cs_{0.7}Co_4Fe_{2.9}$ is broad (open bulks).

From magnetic studies of $K_{0.28}Co_4Fe_{2.76}$ under pressure [Fig. 2(c)] one can conclude about a broad distribution of CoN_nO_{6-n} configurations, similar to those given by the binomial model. For $K_{0.1}Co_4Fe_{2.7}$ the Co/Fe atomic ratio is 1.48, whereas for $K_{0.28}Co_4Fe_{2.76}$ it is 1.45. It is appears a significant difference resulting the appearance of variety of CoN_nO_{6-n} configurations in $K_{0.28}Co_4Fe_{2.76}$. However, the concentration of strong-field configurations to the amount of 10(1)% does not provide a noticeable PIM effect. This observation raises the question of a minimal concentration of diamagnetic species necessary for the PIM effect to take place and the role of cooperativity in the charge transfer process. Another important factor is the concentration of vacancies, causing the flexibility of the crystal lattice.[10–12]

IV. CONCLUSION

Mössbauer and magnetic studies of $K_{0.1}Co_4Fe_{2.7}$, $K_{0.28}Co_4Fe_{2.76}$, and $Cs_{0.7}Co_4Fe_{2.9}$ under applied hydrostatic pressure revealed a pressure-induced electron transfer

$Co^{2+}(S=\frac{3}{2})$-NC-$Fe^{3+}(S=\frac{1}{2}) \rightarrow Co^{3+}(S=0)$-NC-$Fe^{2+}$ $(S=0)$ in all three compounds. We found no evidence of $Co^{2+}(S=\frac{1}{2})$ accompanying the redox process. The presence of residual $Co^{2+}(S=\frac{3}{2})$ ions at pressures of ~10 kbar demonstrates, that (i) there is no charge transfer due to the lack of Fe^{3+} ions in the neighborhood, and (ii) a pressure of up to ~10 kbar is not sufficient to induce a spin transition $S=\frac{3}{2} \rightarrow S=\frac{1}{2}$ at the Co^{2+} sites. Application of hydrostatic pressure provides a method of ''scanning'' the ligand field strength and allows the determination of some important features of the distribution of $CoN_nO_{6-n}(0 \leqslant n \leqslant 6)$ configurations in the three compounds. The absence of a noticeable PIM effect in $K_{0.1}Co_4Fe_{2.7}$ at ambient pressure is explained by the absence of ''strong field'' CoN_6 configurations, and a narrow distribution centered around the most probable CoN_4O_2 configuration. In contrast, the CoN_6 ''strong field'' configurations are present in $Cs_{0.7}Co_4Fe_{2.9}$ and $K_{0.28}Co_4Fe_{2.76}$ at ambient pressure. This enables PIM to occur in $Cs_{0.7}Co_4Fe_{2.9}$, however the concentration of ''strong field'' configurations in $K_{0.28}Co_4Fe_{2.76}$ is not sufficient to allow a noticeable PIM effect. The broadening and randomization of the CoN_nO_{6-n} distribution in $Cs_{0.7}Co_4Fe_{2.9}$ and $K_{0.28}Co_4Fe_{2.76}$ can be assigned to the influence of the alkali metal ions, statistically distributed in the lattice. We intend to examine such broadening effects and their consequences on the appearance of PIM in Prussian blue analogs by studying the photomagnetic properties and the pressure-induced changes of ligand field strength in other MCoFe analogs (M=Na,K,Rb,Cs) and samples prepared by other methods.

*Electronic mail: v.ksenofontov@uni-mainz.de

[1] O. Sato, T. Iyoda, A. Fujishima, and K. Hashimoto, Science **272**, 704 (1996).
[2] M. Verdaguer, Science **272**, 698 (1996).
[3] A. Bleuzen, C. Lomenech, V. Escax, F. Villain, F. Varret, C. Cartier dit Moulin, and M. Verdaguer, JACS **122**, 6648 (2000).
[4] C. Cartier dit Moulin, F. Villain, A. Bleuzen, M.-A. Arrio, P. Sainctavit, C. Lomenech, V. Escax, F. Baudelet, E. Dartyge, J.-J. Gallet, and M. Verdaguer, JACS **122**, 6653 (2000).
[5] V. Escax, A. Bleuzen, C. Cartier dit Moulin, F. Villain, A. Goujon, F. Varret, and M. Verdaguer, JACS **123**, 12536 (2001).
[6] G. Champion, V. Escax, C. Cartier dit Moulin, A. Bleuzen, F. Villain, F. Baudelet, E. Dartyge, and M. Verdaguer, JACS **123**, 12544 (2001).
[7] O. Sato, Y. Einaga, T. Iyoda, A. Fujishima, and K. Hashimoto, J. Electrochem. Soc. **144**, L11 (1997).
[8] O. Sato, Y. Einaga, T. Iyoda, A. Fujishima, and K. Hashimoto, J. Phys. Chem. B **101**, 3903 (1997).
[9] T. Yokoyama, M. Kiguchi, T. Ohta, O. Sato, Y. Einaga, and K. Hashimoto, Phys. Rev. B **60**, 9340 (1999).
[10] D. A. Pejaković, J. L. Manson, J. S. Miller, and A. J. Epstein, Phys. Rev. Lett. **85**, 1994 (2000).
[11] O. Sato, Y. Einaga, A. Fujishima, and K. Hashimoto, Inorg. Chem. **38**, 4405 (1999).
[12] T. Kawamoto, Y. Asai, and S. Abe, Phys. Rev. Lett. **86**, 348 (2001).
[13] A. Goujon, F. Varret, V. Escax, A. Bleuzen, and M. Verdaguer, Polyhedron **20**, 1339 (2001).
[14] S. Ohkoshi and K. Hashimoto in *Magneto-Optics*, edited by S. Sugano and N. Kojima (Springer-Verlag, Heidelberg, 2000), p. 260.
[15] M. Baran, G. G. Levchenko, V. P. Dyakonov, and G. Shymchak, Physica C **241**, 383 (1995); M. Drillon, P. Panissod, P. Rabu, J. Souletie, V. Ksenofontov, and P. Gütlich, Phys. Rev. B **65**, 104404 (2002).
[16] I. N. Nikolaev, L. S. Pavlyukov, and V. P. Mar'in, Zh. Eksp. Teor. Fiz. **69**, 1844 (1975) [Sov. Phys. JETP **42**, 936 (1975)].
[17] K. Lagarec and D. G. Rancourt, Nucl. Instrum. Methods Phys. Res. B **129**, 266 (1997).
[18] V. Gadet, Ph.D. thesis, Université Pierre et Marie Curie, Paris, 1992.
[19] Y. Einaga, O. Sato, T. Iyoda, Y. Kobayashi, F. Ambe, K. Hashimoto, and A. Fujishima, Chem. Lett. **26**, 289 (1977).
[20] D. H. Martin, *Magnetism in Solids* (Iliffe, London, 1967), pp. 205–206. Compounds containing Co^{2+} complexes are not spin-only materials and typically have a moment of $4.5\mu_B$ to $5.2\mu_B$. Corresponding $\chi_m T$ values for remaining Co^{2+} atoms should vary from 3.4 to 4.5 $cm^3\,mol^{-1}\,K$, which is in fair agreement with experimentally observed ones at maximal pressures for all three compounds under study.